

Proceedings of the Korean Nuclear Autumn Meeting  
Yongpyung, Korea, October 2002

## **A Layer-wise Tension Stiffening Model for Inelastic Finite Element Analysis of Moderately Thick Reinforced Concrete Wall-like Structures**

Sang-Jin Lee\*, Hong-Pyo Lee, Jeong-Moon Seo

ISA, Korea Atomic Energy Research Institute  
P.O. Box 105, Yusung, Daejeon, 306-600, South Korea

\*Tel: +82-42-868-2223, Fax: +82-42-868-8256, Email:sjlee@kaeri.re.kr

### **Abstract**

A layer-wise tension stiffening model is introduced to carry out the inelastic finite element (FE) analysis of moderately thick reinforced concrete (RC) structures. The basic idea of the present model is a selective consideration of tension stiffening effect in a certain zone where the effect is assumed to be active. The CEB-FIP recommendation is tentatively used to identify the effective tension stiffening zone. The proposed model is utilized in the framework of the microscopic RC material model with a nine-node degenerated assumed strain shell element. Finally, a numerical example is carried out to evaluate the performance of the present model in inelastic analysis of RC structures.

### **1. Introduction**

The terms ‘tension stiffening’ and ‘strain softening’ seem to make some confusion without a sound understanding of its physical phenomenon. In general, the term ‘tension stiffening’ is considered as the stiffening effect of concrete material after crack formation due to the interaction between the steel bar and the concrete. The strain softening effect may be in general interpreted as the decreasing pattern of concrete strength in RC or plain concrete.

It has been well recognized that both effects are very significant to the RC structures and has been essentially considered in the FE analysis. However, the precise application of tension stiffening effect to the FE model has not been well investigated although various

tension stiffening models [1] have been suggested through relevant experiments.

In this context, a layer-wise tension stiffening model is proposed for the inelastic FE analysis of moderately thick RC structures. The proposed model considers the tension stiffening effect only in the zone where it is in active and the strain softening effect is optionally considered in the zone with which the tension stiffening effect is not directly related. In order to implement this concept, an assumed strain degenerated shell element [2] based on Reissner-Mindlin (RM) assumption [3] is adopted with layered approach [4]. An elasto-plastic and fracture model is used to represent a general material characteristic of concrete in uncracked situation and the material models such as the shear transfer model and tension stiffening model with relevant cracking criteria are adopted to represent the characteristics of cracked concrete. In addition to the concrete material model, the reinforcing bar is represented as a smeared layer in the shell element and a full bond is assumed in the steel-concrete interface.

A wall element of containment building is used to evaluate the performance of the proposed model with different types or levels of tension stiffening effect. The numerical results evaluated in this study is finally provided as a benchmark for the inelastic analysis of moderately thick RC wall structures focusing on the tension stiffening effect.

## 2. Shell Finite Element Formulation

### 2.1 Geometry and Kinematics of Shell Finite Element

In three dimensional space ( $\mathbb{R}^3$ ), the geometry of the shell element can be defined by two vectors at each nodal point. One vector  $\mathbf{X}(\xi_1, \xi_2)$  expresses the positions of the shell mid-surface which could be denoted as  $[(\xi_1, \xi_2) \in A \rightarrow \mathbb{R}^2]$  and the other vector  $\hat{\mathbf{D}}$ , which is called the unit normal vector, expresses any position with a magnitude of thickness between the top surface and the bottom surface of the shell in the thickness direction  $[\xi_3 \in h \rightarrow \mathbb{R}]$ . After FE discretization on the mid-surface of the continuum shell, the initial configuration of the shell element having a constant thickness  $2t$  can be written as

$$\mathbf{X}(\xi_1, \xi_2, \xi_3) = \bar{\mathbf{X}}(\xi_1, \xi_2) + \xi_3 \bar{\mathbf{D}}(\xi_1, \xi_2) = \sum_{a=1}^9 N_a(\xi_1, \xi_2) \left[ \bar{\mathbf{X}}^a + \xi_3 t^a \hat{\mathbf{D}}^a \right] \quad (1)$$

Since the nine-node Lagrangian shell element is adopted in this study, nine position vectors  $\bar{\mathbf{X}}^a$  which have three Cartesian components  $\bar{X}_i^a (i = 1, 3)$  and nine unit normal vectors  $\hat{\mathbf{D}}^a$  are required to express the shell element. These unit normal vectors which are normal to the mid-surface at the nodal points are evaluated as

$$\hat{\mathbf{D}}(\xi_1^a, \xi_2^a) = \hat{\mathbf{D}}^a = \hat{\mathbf{n}}^a / |\hat{\mathbf{n}}^a| \quad (2)$$

in which  $\hat{\mathbf{n}}^a = [\bar{\mathbf{X}}_{,1} \times \bar{\mathbf{X}}_{,2}]_{\xi_1=\xi_1^a, \xi_2=\xi_2^a}$

The displacement field  $\mathbf{u}$  used in the present shell element having five degrees of freedom per node can be defined as

$$\mathbf{u}(\xi_1, \xi_2, \xi_3) = \sum_{a=1}^9 N_a(\xi_1, \xi_2) [\bar{\mathbf{u}}^a + \xi_3 h^a \bar{\mathbf{V}}^a \boldsymbol{\alpha}^a] \quad (3)$$

where the transformation matrix is  $\bar{\mathbf{V}}^a = [\hat{v}_1^a, \hat{v}_2^a]$ , the translation vector is  $\mathbf{u}^a = [u_1^a, u_2^a, u_3^a]^T$  and the rotation vector is  $\boldsymbol{\alpha}^a = [\alpha_1^a, \alpha_2^a]$

Note that the above displacement expression is used for the original Ahmad shell element [5] and in particular the nodal coordinate system is adopted to express the rotational displacement at each node.

## 2.2 Strain definition

In this study, the standard strain-displacement matrix is substituted with assumed strains to alleviate the element deficiencies inherited in the degenerated RM shell element. The sampling points used in the formulation of assumed natural strains are presented in Figure 1.

The interpolation functions used in formulating the assumed strains are based on Lagrangian interpolation polynomials as proposed by Huang and Hinton [6]. Consequently, the substitute assumed natural strains  $\hat{\boldsymbol{\varepsilon}}$  can be defined in the following form:

$$\begin{aligned} \hat{\varepsilon}_{11} &= \sum_{i=1}^2 \sum_{j=1}^3 \mathcal{P}_i(\xi_1) \mathcal{Q}_j(\xi_2) \varepsilon_{11}^{(\delta)}; & \hat{\varepsilon}_{22} &= \sum_{i=1}^2 \sum_{j=1}^3 \mathcal{P}_i(\xi_2) \mathcal{Q}_j(\xi_1) \varepsilon_{22}^{(\delta)} \\ \hat{\varepsilon}_{12} &= \sum_{i=1}^2 \sum_{j=1}^2 \mathcal{P}_i(\xi_1) \mathcal{P}_j(\xi_2) \varepsilon_{12}^{(\delta)} \\ \hat{\varepsilon}_{13} &= \sum_{i=1}^2 \sum_{j=1}^3 \mathcal{P}_i(\xi_1) \mathcal{Q}_j(\xi_2) \varepsilon_{13}^{(\delta)}; & \hat{\varepsilon}_{23} &= \sum_{i=1}^2 \sum_{j=1}^3 \mathcal{P}_i(\xi_2) \mathcal{Q}_j(\xi_1) \varepsilon_{23}^{(\delta)} \end{aligned} \quad (4)$$

in which  $\delta = 2(j-1) + i$  denotes the position of the sampling point as shown in Figure 1 and the shape functions  $\mathcal{P}_i(\xi)$  and  $\mathcal{Q}_i(\xi)$  are

$$\begin{aligned} \mathcal{P}_1(\xi) &= \frac{1}{2}(1 + \sqrt{3}\xi), & \mathcal{P}_2(\xi) &= \frac{1}{2}(1 - \sqrt{3}\xi) \\ \mathcal{Q}_1(\xi) &= \frac{1}{2}\xi(\xi + 1), & \mathcal{Q}_2(\xi) &= 1 - \xi^2, & \mathcal{Q}_3(\xi) &= \frac{1}{2}\xi(\xi - 1) \end{aligned} \quad (5)$$

The assumed strains  $\hat{\varepsilon}$  derived from (4) are used in the present shell element instead of the strains  $\varepsilon$  which is consistently obtained from the displacement field of (3). Note that the geometrically linear strain terms are only used in this study.

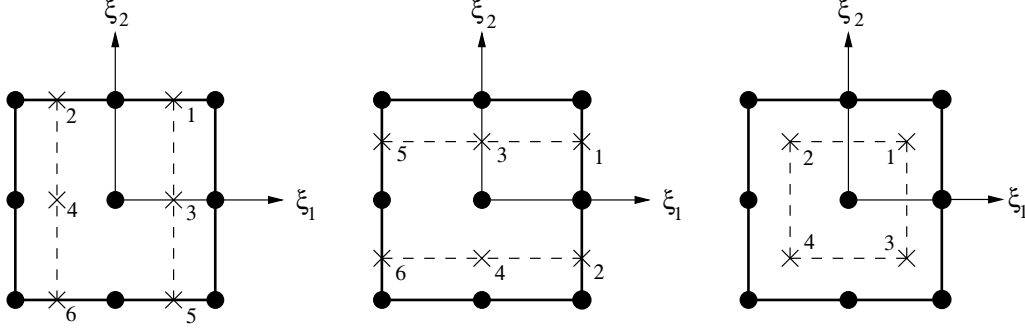


Figure 1: The sampling points for the assumed strains; left for  $\hat{\varepsilon}_{11}, \hat{\varepsilon}_{13}$ , centre for  $\hat{\varepsilon}_{22}, \hat{\varepsilon}_{23}$  and right for  $\hat{\varepsilon}_{12}$

### 2.3 Constitutive Equation

The so-called elasto-plastic fracture model [7] is adopted for uncracked concrete in this study. It uses an equivalent stress-strain relationship to determine the concrete stress level due to the external load. With isotropic material assumption, the constitutive equation for uncracked concrete can be written as follows

$$\mathbf{D}_p^* = \begin{bmatrix} \bar{\lambda}(E^*, \nu) + 2\mu(E^*, \nu) & \bar{\lambda}(E^*, \nu) & 0 \\ \bar{\lambda}(E^*, \nu) & \bar{\lambda}(E^*, \nu) + 2\mu(E^*, \nu) & 0 \\ 0 & 0 & \mu(E^*, \nu) \end{bmatrix}; \quad \mathbf{D}_s^* = \mathbf{D}_s \quad (6)$$

where the parameter  $\bar{\lambda} = \frac{\nu E^*}{1-\nu^2}$  is the reduced Lamé's constant for the generalized plane stress-strain relationship and  $\mu = G = \frac{k_s E^*}{2(1+\nu)}$  is the shear modulus in which  $k_s$  is the shear correction factor which is taken as 5/6 and  $\nu$  is the Poisson ratio. The modulus  $E^*$  can be calculated by using the equivalent stress-strain relationship [7]:

$$E^* = \begin{cases} E_c f_c (\bar{\varepsilon}_e \dot{K}_o + \dot{\bar{\varepsilon}}_e K_o) & : \text{loading condition} \\ E_c & : \text{unloading condition} \end{cases} \quad (7)$$

in which the  $f_c$  is the compressive strength of concrete,  $\bar{\varepsilon}_e (= \bar{\varepsilon} - \bar{\varepsilon}_p)$  is the equivalent elastic strain and the fracture parameter  $K_o = e^p$  is formulated by the experimental data. The exponent is defined as  $p = e^{-0.73 \bar{\varepsilon}_{max}} [1 - e^{-1.25 \bar{\varepsilon}_{max}}]$  in which  $\bar{\varepsilon}_{max}$  is the maximum experienced value of the equivalent strain during the analysis.

However, the concrete will have a material axis after crack formation and another constitutive equation is therefore required to represent the characteristics of cracked concrete. Since cracked concrete does not have any rigidity in the direction normal to crack, the constitutive equation for cracked concrete associated with the material axis can be defined as

$$\hat{\mathbf{D}}_p^* = \begin{bmatrix} \hat{D}_1^* & 0 & 0 \\ 0 & \hat{D}_2^* & 0 \\ 0 & 0 & \hat{D}_{12}^* \end{bmatrix}; \quad \hat{\mathbf{D}}_s^* = \begin{bmatrix} \hat{G}_{cr}^* & 0 \\ 0 & \hat{G}_{cr}^* \end{bmatrix} \quad (8)$$

where the in-plane rigidity matrix component are

$$\hat{D}_i^* = \begin{cases} \hat{D}_{it}^* = \begin{cases} 2f_t/\varepsilon_{cr} & \varepsilon < \frac{1}{2}\varepsilon_{cr} \\ 0 & \varepsilon > \frac{1}{2}\varepsilon_{cr} \end{cases} & : \text{tension} \\ \hat{D}_{ic}^* = -E_c f_c (\varepsilon_e \dot{K}_o + \dot{\varepsilon}_e K_o) & : \text{compression} \end{cases} \quad (9)$$

$$\hat{D}_{12}^* = \frac{1}{1/G_{st}^{(1)} + 1/G}$$

in which  $f_t$  is the tensile strength of concrete,  $\varepsilon_{cr}$  is cracking tensile strain,  $G_{st}^{(1)} = f_{st}\delta/(\delta^2 + \omega^2)$  in which  $f_{st} = 18.0f_c^{\frac{1}{3}}$ ,  $\delta$  is the shear slip displacement and  $\omega$  is the crack width. Transverse shear rigidity matrix component  $\hat{G}_{cr}$  is

$$\hat{G}_{cr} = \frac{1}{1/G_{st}^{(2)} + 1/G} \quad (10)$$

where  $G_{st}^{(2)} = 36/\varepsilon_t$  in which  $\varepsilon_t$  is the tensile strain normal to crack plane. Note that the term  $\hat{D}_{it}^*$  will cooperate with the tension stiffening model in cracked situation.

As cracking criteria, Niwa's model and Aoyagi-Yamada's model [8, 9] are used in tension-compression region and tension-tension stress region respectively. Although the stress-based cracking criteria is adopted in this study, crack formation will be confirmed with the satisfaction of two conditions: stress level reaches the adopted cracking criteria and principal strain meets the given limited strain values. Since the constitutive equation is formulated in associated with the material axis, the transformation scheme between the material axis and shell local coordinate system is used.

Besides, a reinforcing bar is represented as a smeared layer in the shell element. The bi-linear stress-strain relationship [10] is used to represent the material characteristic of steel reinforcement embedded in the concrete such as

$$\sigma_s = \sigma_{sy} + E_{sh}(\varepsilon_s - \varepsilon_{sy}) \quad (11)$$

where  $\sigma_s$  is the average stress,  $\varepsilon_s$  is average strain,  $\sigma_{sy}$ ,  $\varepsilon_{sy}$  are the stress and strain values, respectively, where the hardening starts. The hardening rate of the steel  $E_{sh}$  is explained in Reference [10].

On the other hand, if the reinforcement yields at the crack plan, the average stress and strain will drift away from the elastic region although other parts of the reinforcement have still not yielded. At this point, average stress will be lower than yield strength. Therefore, the yielding of reinforcement will be confirmed when the overall tensile strength of reinforcement is reduced or the stress level of reinforcement reaches yield strength during the analysis.

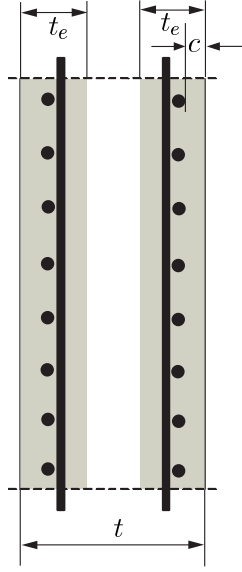
### 3. Layer-wise Tension Stiffening Model

As well known fact, the formation of primary crack is characterized by a drop of the stress level in concrete to zero. However, the concrete between the cracks still carries tensile stress because the bond slip exists between the intact concrete and steel. This load-carrying capacity in cracked concrete is called tension stiffening. However, there may exist a zone emancipated from the tension stiffening effect in a certain structure such as moderately thick RC wall-like structure. It implies that uniform application of tension stiffening effect to the whole structure through the thickness direction may deliver stiffer numerical solution. In this context, the tension stiffening effect should be considered only in the zone where the tension stiffening effect really exists. Therefore, we introduced a layer-wise tension stiffening model which apply tension stiffening effect only to the selected layer in the thickness direction of the structures.

To achieve this model, the identification of effective tension stiffening zone is necessarily required. In this study, we adopt the CEB-FIP recommendation [11] which uses the concrete cover  $c$  and the diameter of the steel reinforcement  $\phi_s$  as key parameters as shown in Figure 2.

Once the effective tension stiffening zone is decided, we can prepare the FE model by using the layer approach. At this stage, we also have to decide whether or not the strain softening effect will be considered in the zone where the tension stiffening is not effective. Therefore, the present model can have three options in the FE analysis:

- full consideration of the tension stiffening effect in the whole structure
- selective consideration of the tension stiffening effect in active zone without strain softening effect
- selective consideration of the tension stiffening effect in active zone with strain softening effect



$$t_e = \min \left\{ 2.5 \left( c + \frac{\phi_s}{2} \right), \frac{t}{2} \right\}$$

$$\phi_s = \frac{\phi_h \rho_h + \phi_m \rho_m}{\rho_h + \rho_m}$$

$t_e$  : effective tension stiffening zone

$c$  : concrete cover

$\phi_s$  : average diameter of steel bar in panel

$\phi_h$  : diameter of steel bar in hoop direction

$\phi_m$  : diameter of steel bar in meridional direction

$\rho_h$  : reinforcement ratio in hoop direction

$\rho_m$  : reinforcement ratio in meridional direction

Figure 2: The evaluation of effective tension stiffening zone

Now, the choice of the adequate tension stiffening and strain softening models is required. In this study, the tension stiffening effect is considered in the exponential form as follow (See Figure 3)

$$\sigma = f_t \left( \frac{\varepsilon_{cr}}{\varepsilon} \right)^\beta \quad (12)$$

where,  $f_t$  is the tensile strength of concrete,  $\varepsilon_{cr}$  is cracking tensile strain and  $\varepsilon$  is the current strain level.

However, the tension stiffening model due to the bond may not be appropriate for the zone filled with plain concrete, so that the fracture mechanics approach is adopted to model the concrete. More specifically, the fracture energy release rate  $G_f$  is adopted to represent the material characteristic of the concrete.

Assuming that the stress  $\sigma$  across an open crack is a function of the crack width  $w$ , the fracture energy is defined as

$$G_f = \int_0^\infty \sigma(w) dw \quad (13)$$

where  $G_f$  represents the energy required to create the crack.

In the smeared crack approach, the so-called characteristic length  $\ell_c$  [12] is used to evaluate the softening parameter  $\alpha$  such as

$$\alpha = \frac{G_f}{f_t \ell_c} \quad (14)$$

The strain softening effect curve is then assumed to be an exponential function (See Figure 3)

$$\sigma = f_t e^{\frac{1}{\alpha}(\epsilon_{cr} - \epsilon)} \quad (15)$$

where  $f_t$  is the tensile strength of concrete,  $\epsilon_{cr}$  is strain at cracking,  $\alpha$  is the softening parameter of (14), and  $\epsilon$  is the nominal tensile strain in the cracked zone.

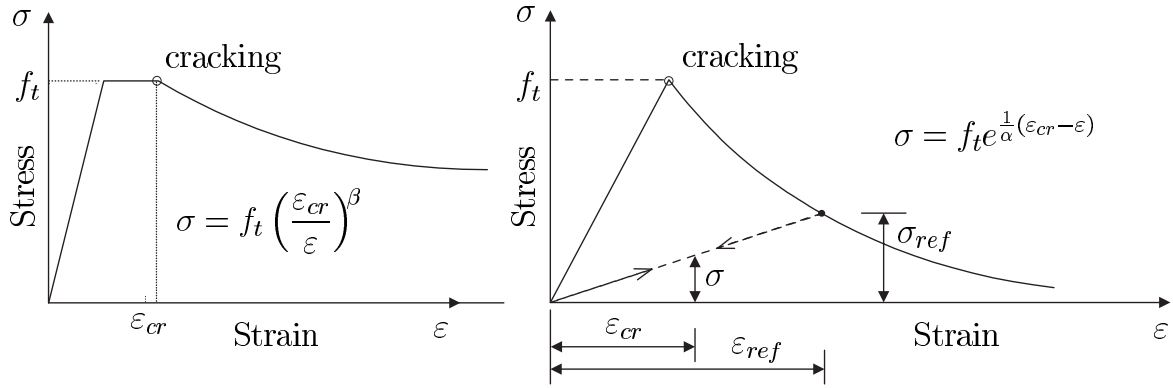


Figure 3: (left) Tension stiffening model and (right) strain softening model

The shell element can now use an appropriate material model described in this section in layer-wise manner.

#### 4. Numerical Test

A wall element of containment building is used to evaluate the performance of the proposed model. The wall element was originally tested by CTL(Construction Technology Laboratories) as part of an EPRI(Electric Power Research Institute) program to provide a experiment-verified numerical method for estimating capacities of concrete reactor containment buildings under internal over-pressurization. A detailed description of the experiment refers to the report [13] produced by CTL and a brief summary of the experiment is therefore provided here. All eight specimens were used in the experiment. Among them, the six specimens were produced with typical size and typical space of reinforcement used in RC containment design. The wall specimen BA1 out of those six typical ones, which do not have diagonal reinforcement and is comparable to the reinforcement ratio used in the wall of RC containment buildings, is eventually adopted for numerical test.

The geometry and layout of steel reinforcement of the wall BA1 is described in Figure 4. The wall has the size of  $60in. \times 60in. \times 24in.$  ( $1524mm \times 1524mm \times 610mm$ ) and a mat of steel reinforcement is placed in each face of the wall. The reinforcement is placed with the equal space of  $12in.$  ( $305mm$ ) and has a minimum clear cover of  $2in.$  ( $50mm$ ). The hoop and meridional reinforcement ratios are  $\rho^{(h)} = A_s^{(h)}/A_g = 0.022$  and  $\rho^{(m)} = A_s^{(m)}/A_g = 0.013$  respectively, where  $A_s^{(h)}$  is the total area of hoop reinforcement,  $A_s^{(m)}$  is the total area of meridional reinforcement and  $A_g$  is the gross cross-sectional area of the wall.

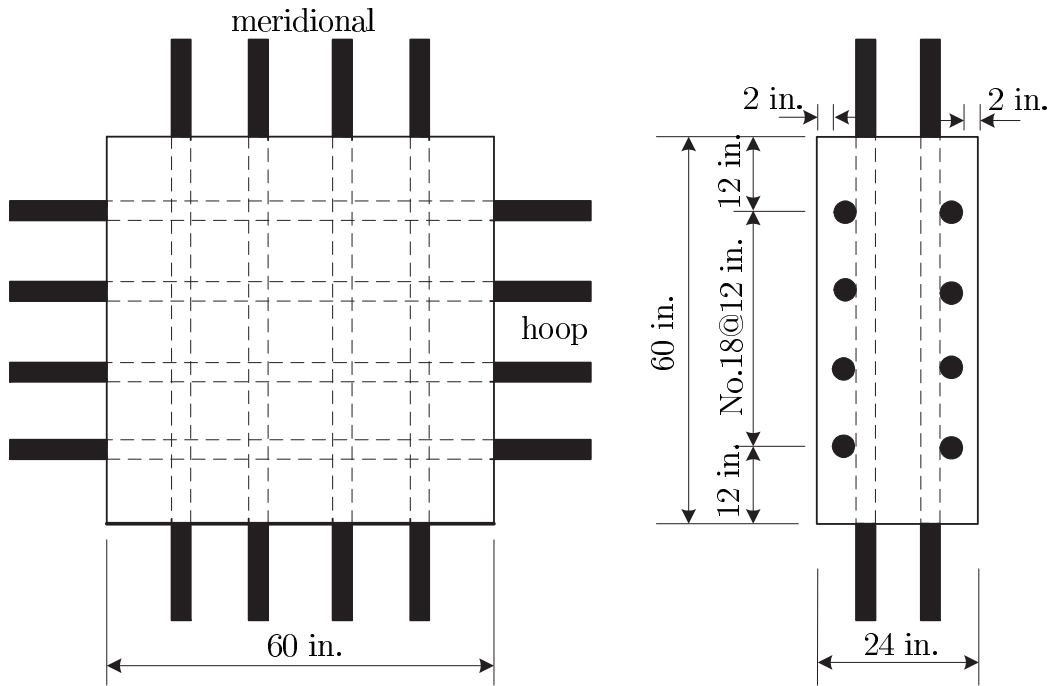


Figure 4: The wall element BA1 tested in CTL

The biaxial load is applied to the wall with the ratio 2 : 1 in the hoop and meridional direction. The material properties of concrete and steel reinforcement used in the wall are given in Table 1.

Table 1: Material properties used in the wall ( $kg/cm^2$ )

Designation	direction	steel		concrete			
		$E_s$	$f_y$	$E_c$	$f_c$	$f_t$	$\nu$
BA1	hoop	2235858	4774.1	248686.5	252.1	35.6	0.2
	meridional	1926494	4809.2	-	-	-	-

The effective tension stiffening zone is calculated by using the CEB-FIB recommenda-

tion [11] and the  $2 \times 2$  FE mesh is created with the value of effective tension stiffening zone  $t_e = 19\text{cm}$ . As mentioned in Section 3, three options can be used in the present layer-wise tension stiffening model. However, it should be noted that the first and the second options are numerically tested in this study although all three options are suggested in this paper.

As the first case of numerical test, we consider the tension stiffening effect in whole structures with the value of tension stiffening parameter  $\beta = 0.4$  which is recommended for deformed bar in Reference [7]. From the numerical result of this case, a great discrepancy is detected between the present result and the experimental result provided by CTL. More specifically, the tension stiffening effect is greatly overestimated as shown in Figure 5(top). In particular, the cracking stress level obtained from the numerical test is almost three times higher than the value obtained from the experiment. Therefore, the lower value of tensile strength is experimentally adopted to produce the comparative results. As the second case, two tensile strengths of concrete,  $f_t = 12.6, 22.6\text{kg/cm}^2$ , are tested with the same tension stiffening parameter  $\beta = 0.4$  and the result are illustrated in Figure 5(down). From numerical result, the solution obtained with the tensile strength  $f_t = 12.6\text{kg/cm}^2$  is very close to the experimental solution. However, at this stage we also find that the numerical solution with  $f_t = 35.6\text{kg/cm}^2$  has a good agreement with the another experimental solution [14] obtained with a similar specimen to CTL's. Therefore, we reaches tentative conclusion that the experiment might have some error. We then decided to provide the numerical reference solution and compare it with the stress level of the bare bar used in the wall BA1.

In order to produce the reference solution, the layer-wise tension stiffening with the parameters ( $\beta = 0.4$ ) are now used as the third case of numerical test. As shown in Figure 6, the layer-wise tension stiffening model produces much accurate stress-strain curve especially after crack formation in concrete. In other words, Too high stress level after concrete cracking and even after the yielding of the steel bar, which is one of the major drawback due to the full consideration of tension stiffening effect in whole thickness, disappear with the use of the proposed layer-wise tension stiffening model.

## 5. Concluding Remarks

A layer-wise tension stiffening model is proposed for a moderately thick RC wall-like structures. The model is implemented in a nine-node assumed strain degenerated shell element with microscopic concrete material model. The proposed tension stiffening model is tested in the wall element of containment building and the numerical result is suggested as new reference solution for inelastic FE analysis of RC structures focusing on tension stiffening effect. From this study, we found a possible error in the CTL's experiment and also an excellent performance of the proposed model. The proposed model can predict the inelastic behaviour of the wall element very accurately in whole range of loading process

and show a great possibility to be used in various forms of RC structures.

## Acknowledgement

The research grant from the Ministry of Science and Technology, Korea, for the Nuclear Research & Development Program is gratefully acknowledged.

## References

- [1] Hsu, T.T.C. and Ahang, L.X., Tension stiffening in reinforced concrete membrane elements, *ACI Structural Journal*, Vol.93, pp.108-115, 1996
- [2] Lee, S.J. and Kanok-Nuchulchai, W., A nine-node assumed strain finite element for large deformation analysis of laminated shells, *Int. J. Numer. Meth. Engng.*, Vol.42, pp.777-798, 1998
- [3] Reissner, E., The effect of transverse shear deformation on the bending of elastic plate, *ASME, J. Appl. Mech.*, Vol.12, pp.69-76, 1945
- [4] Hinton, E and Owen, D.R.J., *Finite element software for plates and shells*, Pineridge Press, Swansea, 1984
- [5] Ahmad, S., Irons, B.M. and Zienkiewicz, O.C., Analysis of thick and thin shell structures by curved finite elements, *Int. J. Numer. Meth. Engng.*, Vol.2, pp.419-451, 1970
- [6] Huang, H.C. and Hinton, E., A new nine-node degenerated shell element with enhanced membrane and shear interpolation, *Int. J. Numer. Meth. Engng.*, Vol.22, pp.73-92, 1986
- [7] Maekawa, K. and Okamura, H., The deformation behaviour and constitutive equation concrete using Elasto-Plastic and Fracture Model, *Journal of faculty of Engineering, University of Tokyo (B)*, Vol. 37, No. 2, pp.253-328, 1983
- [8] Niwa, K., The structural characteristic of reinforced concrete panel, Msc. thesis, Department of civil engineering, University of Tokyo, 1980
- [9] Aoyagi, Y. and Yamada, K., Strangth and deformation characteristics of RC shell elements subjected to in-plane forces, *Concrete library international JSCE*, No.4, pp.129-160, 1984

- [10] Shima, H., Chou, L. and Okamura, H., Micro and Macro models for bond behaviour in reinforced concrete, *Journal of faculty of Engineering, University of Tokyo (B)*, Vol.39, No.2, pp.133-194, 1987
- [11] CEB-FIP. Model Code 1990, Bulletin d'Information. CEB, Lausanne, Switzerland, 1990
- [12] Bangashi, M.Y.H, *Concrete and concrete structures: numerical modelling and applications*, Elsevier Applied Science, 1989
- [13] Julien, J.T., Schultz, D.M. and Weinmann, T.L., Concrete Containment Structural Element Tests, Volumn 1 & 2, Construction Technology Laboratories, 1984
- [14] Kim, N.S., Seo, J.W., Cho, N.S., Koo, E.S. and Cho, J.Y., Structural member tests of the prestress concrete containment, KAERI/CM-493/2001, KAERI, 2001

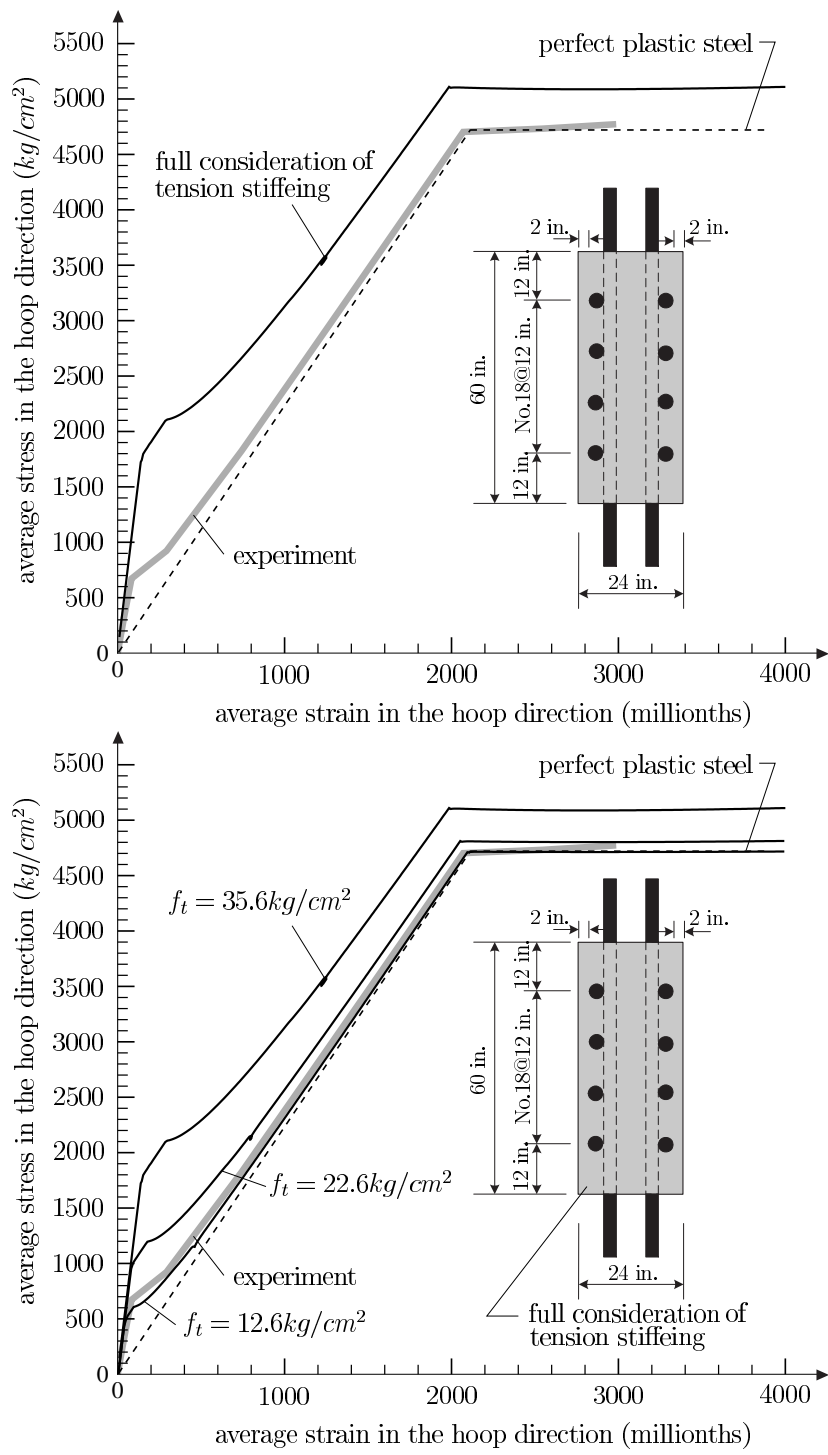


Figure 5: The result with full consideration of tension stiffening

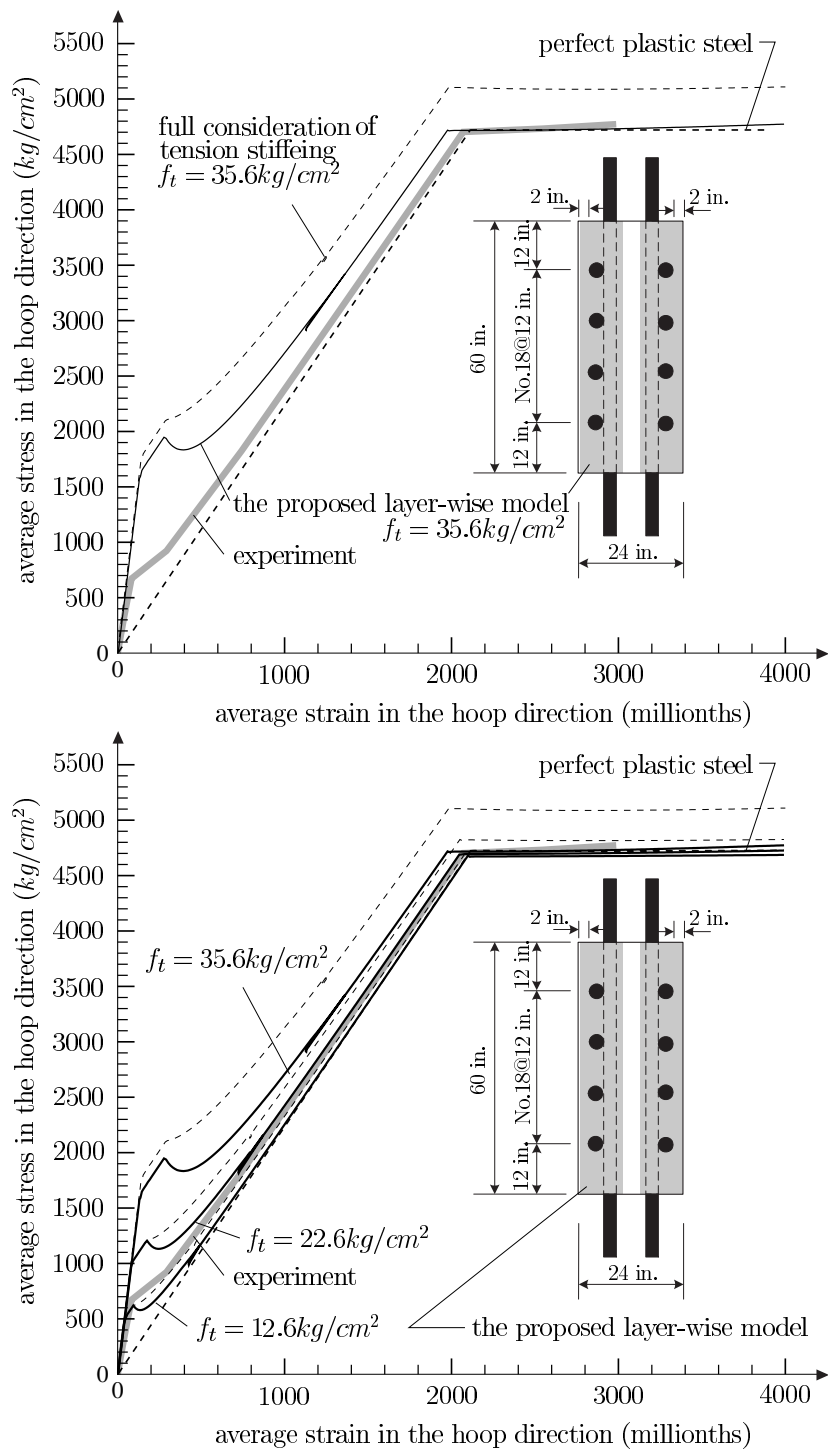


Figure 6: The result with a proposed model